EPIPOLAR-PLANE IMAGE ANALYSIS: A TECHNIQUE FOR ANALYZING MOTION SEQUENCES

Robert C. Bolles
H. Harlyn Baker

Reprinted from PROCEEDINGS OF THE IEEE THIRD WORKSHOP
ON COMPUTER VISION: REPRESENTATION AND CONTROL,
Bellaire, Michigan, October 13-16, 1985

IEEE COMPUTER SOCIETY
1730 Massachusetts Avenue, N.W.
Washington, D.C. 20036-1903

IEEE
COMPUTER
SOCIETY
PRESS

THE INSTITUTE OF ELECTRICAL AND EL

EPIPOLAR-PLANE IMAGE ANALYSIS: A TECHNIQUE FOR ANALYZING MOTION SEQUENCES*

Robert C. Bolles
H. Harlyn Baker
SRI International
333 Ravenswood Avenue
Menlo Park, CA 94025.

Abstract

A technique for unifying spatial and temporal analysis of an image sequence taken by a camera moving in a straight line is presented. The technique is based on a "dense" sequence of images–images taken close enough together to form a solid block of data. Slices of this solid directly encode changes due to motion of the camera. These slices, which have one spatial dimension and one temporal dimension, are more structured than conventional images. This additional structure makes them easier to analyze. We present the theory behind this technique, describe an initial implementation, and discuss our preliminary results.

Introduction

Most motion-detection techniques analyze pairs of images, and hence are fundamentally similar to conventional stereo techniques (e.g., [1], [5], and [6]). A few researchers have considered sequences of three or more images (e.g., [8], [10], and [11]), but still the process is one of matching discrete items at discrete times. And yet, it is widely acknowledged that there is a potential benefit from unifying the analysis of spatial and temporal information. In this paper we present a technique to perform this type of unification for straight-line motions.

Motion-analysis techniques using pairs or triples of images are designed to process images that contain significant changes from one to another – features may move more than 20 pixels between views. These large changes force the techniques to tackle the difficult problem of stereo correspondence (Figure 1 shows an image triple with a typical inter-frame separation). Our idea, on the other hand, is to take a sequence of images from positions that are very close together – close enough that almost nothing changes from one image to the next. In particular, we take images close enough together that none of the image features moves more than a pixel or so (Figure 2 shows the first three images from one of our sequences containing 125 images). This sampling frequency guarantees a continuity in the temporal domain that is similar to continuity in the spatial domain. Thus, an edge of an object in one image appears temporally adjacent to (within a pixel of) its occurrence in both the preceding and following images. This temporal continuity makes it possible to construct a solid of data in which time is the third dimension and continuity is maintained over all three dimensions (see Figure 3). This solid of data is referred to as *spatio-temporal data.*

The traditional motion-analysis paradigm detects features in spatial images (i.e., the *uv* images in Figure 3), matches them from image to image, and then deduces the motion. We, however, propose an approach that is orthogonal to this. We suggest slicing the spatio-temporal data along a temporal dimension (see Figure 4), locating features in these slices, and then computing three-dimensional locations. Our reasoning is that the temporal image slices can be formed in such a way that they contain more structure than spatial images; thus, they are more predictable and, hence, easier to analyze.

To convince you of the utility of this approach, we must demonstrate that there is an interesting class of motions for which we can build structured temporal images. In the next section we show that this can be done whenever the camera moves in a straight line. We call these temporal images *epipolar-plane images,* or EPIs, from their geometric properties. In Section 3 we describe the results of our experiments in computing the depths of objects from their paths through the EPIs. And finally, in Section 4 we discuss the strengths and weaknesses of the technique and outline some current and future directions for our work.

Epipolar-Plane Images

In this section we define an epipolar-plane image (an EPI) and explain our interest in it. First, however, we review some stereo terminology. Consider Figure 5, which is a diagram of a general stereo configuration. The two cameras are modeled as pin-holes with the image planes in front of the lenses. For each point P in the scene, there is a plane, called the *epipolar plane,* which passes through the point and the line joining the two lens centers. This plane intersects the two image planes along *epipolar lines.* All the points in the epipolar plane are projected onto one epipolar line in the first image and a corresponding epipolar line in the second image. The importance of these lines for stereo processing is that they reduce the search required to find matching points from two dimensions to one. Thus, to find a match for a point along one epipolar line in an image it is only necessary to search along the corresponding epipolar line in the other image. This is termed the *epipolar constraint.*

One further definition that is essential to understanding our approach is that of an *epipole.* An *epipole* in a stereo configuration is the intersection of the line joining the lens centers and an image plane (see Figure 5). In motion analysis, an epipole is often referred to as a focus of expansion (FOE) because the epipolar lines radiate from it.

*This research was supported by DARPA Contracts MDA 903-83-C-0027 and DACA 76-85-C-0004

0-8186-0685-1/85/0000/0168$01.00

Consider a simple motion in which a camera moves from right to left, with its optical axis orthogonal to its direction of motion (see Figure 6). For this type of motion the epipolar plane for a point, such as P, is the same for all pairs of camera positions, and we refer to that plane as the epipolar plane for P for the whole motion.

The epipolar lines associated with one of these epipolar planes are horizontal scan lines in the images (see Figure 6). The projection of P onto these epipolar lines moves to the right as the camera moves to the left. The velocity of this movement along the epipolar line is a function of P's distance from the line joining the lens centers. The closer it is, the faster it moves.

For this motion, the epipolar lines are not only horizontal, they occur at the same vertical position in all the images. Therefore, a horizontal slice of the spatio-temporal data formed from this motion contains all the epipolar lines associated with one epipolar plane (see Figure 7).

Figure 7 shows three of the images used to form the solid of data. Typically a hundred or more images are used, making P's trajectory through the data a continuous path, as indicated in the diagram. For this type of lateral motion, if the camera moves a constant distance between images, the trajectories are straight lines (see Appendix A).

Figure 8 shows a horizontal slice through the solid of data shown in Figure 3, which was constructed from a sequence of 125 images taken by a camera moving from right to left. Figure 9 shows a frontal view of that slice. We call this type of image an epipolar-plane image (EPI) because it is composed of one-dimensional projections of the world points lying on an epipolar plane. Each horizontal line of the image is one of these projections. Thus, time progresses from bottom to top, and, as the camera moves to the left, the features move to the right.

There are several things to notice about this image. First, it contains only linear structures. In this respect it is much simpler than the spatial images used to create it (see Figure 1 for comparison). Second, the slopes of the lines determine the distances to the corresponding features in the world. The greater the slope, the farther the feature. Third, occlusion, which occurs when a closer feature moves in front of a more distant one, is immediately apparent in this representation. For example, the narrow white bar at the left center of the EPI in Figure 9 is initially occluded, then it is visible for a while until it is occluded briefly by a thin light object, then visible again before being rapidly occluded twice by two darker objects, and then is continuously visible until the end of the sequence. Thus, the same object is seen four different times.

Figure 10 shows another EPI sliced from the data in Figure 3. Its basic structure is the same as Figure 9; however, it illustrates the variety of patterns that can occur in an EPI.

The EPIs in Figures 9 and 10 were constructed from a simple right-to-left motion with the camera oriented at right angles to the motion. For what other types of motions can EPIs be constructed? The answer is that they can be constructed for any straight-line motion. As long as the lens center of the camera moves in a straight line the epipolar planes remain fixed relative to the scene. The points in each of these planes function as a unit. They are projected onto one line in the first image, another line in the second image, and so on. The camera can even change its orientation about its lens center as it moves along the line without affecting this partitioning of the scene. Orientation changes move the epipolar lines around in the image plane, significantly complicating the construction of the EPIs, but the epipolar planes remain unchanged since the line joining the lens centers remains fixed.

Figure 11 is an EPI formed from a sequence of images taken by a camera moving forward and looking straight ahead. Again the image is very structured, except that, instead of lines, it is composed of curves. For this type of motion, in fact for any straight-line motion in which the camera is at a fixed orientation relative to the direction of motion (see Figure 12), the trajectories in the EPI's are hyperbolas (see Appendix B). But not only are they hyperbolas, they are simple hyperbolas in the sense that their asymptotes are vertical and horizontal lines. A right-to-left motion, such as the one mentioned above, is just a special case in which the hyperbolas degenerate into lines.

If the lens center does not move in a line, the epipolar planes passing through a world point differ from one camera position to the next. The points in the scene are grouped one way for one pair of camera positions and a different way for another pair of positions. This makes it impossible to partition the scene into a fixed set of planes, which in turn means that it is not possible to construct EPIs for such a motion.

One last observation about EPIs: since an EPI contains all the information about the features in a slice of the world, the analysis of a scene can be partitioned into a set of analyses, one for each slice. In the case of a right-to-left motion, there is one analysis for each scanline in the image sequence. This ability to partition the analysis is one of the key properties of our motion-analysis technique. Slices of the spatio-temporal data can be analyzed independently (and possibly in parallel), and then the results can be combined into a three-dimensional rep-

Experimental Results

We have implemented a program that computes three-dimensional locations of world features by analyzing EPIs constructed from right-to-left motions. The program currently consists of the following steps:

1. 3D smoothing of the spatio-temporal data
2. Slicing the data into EPIs
3. Detecting edges, peaks, and troughs
4. Segmenting edges into linear features
5. Merging collinear features
6. Computing x-y-z coordinates
7. Building a map of free space
8. Linking x-y-z points between EPIs

In this section we illustrate the behavior of this program by applying it to the data shown in Figure 3.

The first step smooths the three-dimensional data to reduce the effects of noise and camera jitter, and to determine the temporal contours subsequently to be used as features. This is done by applying a sequence of three one-dimensional Gaussians ([3] and [4] explore other uses of spatio-temporal convolution).

The second step forms EPIs from the spatio-temporal data. For a lateral motion this is straightforward because the EPIs are horizontal slices of the data. Figure 9 shows the EPI selected to illustrate steps three through seven.

The third step detects edge-like features in the EPI. It currently locates four types of features: positive and negative zero-crossings [7] and peaks and troughs in the difference of Gaussians. The zero-crossings indicate places in the EPI where there is a sharp change in image intensity, typically at surface boundaries or surface markings, and the peaks/troughs occur between these zero-crossings. The former are generally more precisely positioned than the latter. Figure 13 shows all four types of features detected in the EPI shown in Figure 9.

The fourth step fits linear segments to the edges. It does this in two passes. The first pass partitions the edges at sharp corners by analyzing curvature estimates along the edges. The second pass applies Ramer's algorithm [9] to recursively partition the smooth segments into line segments. Figure 14 shows the line segments derived from the edges in Figure 13.

The fifth step builds a description of the line segments that links together those that are collinear. The intent is to identify sets of lines that belong to the same feature in the world. By bridging gaps caused by occlusions, the program can improve its estimates of the features' locations as well as extract clues about the nature of the surfaces in the scene. The program only links together features of the same type, except that positive and negative zero crossings may be joined, since the contrast across an edge can differ from one view to the next. Figure 15 shows the peak features from Figure 14 that are linked together by the program.

The line intersections in Figures 14 and 15 indicate temporal occlusions. For each intersection, the feature with the smaller slope is the one that occludes the other.

The sixth step computes the x-y-z locations of the world features corresponding to the EPI features. The world coordinates are uniquely determined by the location of the epipolar plane associated with the EPI and the slope and intercept of the line in the EPI. To display these three-dimensional locations, the program plots the two-dimensional coordinates of the features in the epipolar plane. Figure 16 shows the epipolar plane coordinates for the features shown in Figure 14. The shape and size of each ellipse depicts the error associated with the feature's location (this depends on the length of the line and the variance of the fit).

The seventh step builds a two-dimensional map of the world that indicates which areas are empty. The idea behind this construction is that, whenever a feature is seen by the camera, there is a clear line of sight from the camera to the feature. Therefore, if a feature is visible continuously during a portion of a motion, this line of sight sweeps out a triangle of empty space defined by the feature's location, the first position of the camera at which the feature is visible, and the last position at which the feature is visible. The program builds the map of empty space by constructing one of these triangular regions for each line segment found in an EPI, and then OR-ing them together. Figure 17 shows the map constructed for the features in Figure 16.

Figures 18 through 21 show the processing for the EPI 30 lines from the bottom of the uv images. This slice contains a plant on the left, a shirt draped over a chair, part of the top of a table, and in the right foreground, a ladder.

Figures 22 and 23 are stereo (crossed-eye) displays, showing some preliminary results in the eighth step of our analysis - combining the spatial data from the individual EPIs. Figure 22 shows the full set of x-y-z points. The display is fairly dense, since all points, including those arising from very short segments, are depicted. For spatial continuity, we link points between the various EPIs (nearest neighbors in overlapping error ellipses). Figure 23 displays those whose connected length is greater than 2.

Discussion

The following positive characteristics of this approach should be noted:

- Spatial and temporal data are treated together as a single unit;
- The acquisition and tracking steps of the conventional motion analysis paradigm are merged into one step;
- The approach is feature-based, but is not restricted to point features – linear features that are perpendicular to the direction of motion can also be used;
- There is more structure in an EPI than in a standard spatial image, which means that it is easier to analyze, and hence easier to interpret;
- Occlusion is manifested in an EPI in a way that increases the chance of detection because the edge is viewed over time against a variety of backgrounds;
- EPIs facilitate the segmentation of a scene into opaque objects occurring at different depths because they encode a *homogeneous* slice of the object over time;
- There are some obvious ways to make the analysis incremental in time, and partitionable in y (epipolar planes), for high speed performance.

With these benefits, the inherent limitations and current restrictions must be borne in mind:

- Motion must be in a straight line and (currently) the camera must be at a fixed angle relative to the direction of motion;
- Frame rate must be high enough to limit the frame-to-frame changes to a pixel or so (more specifically, such that the projective width of a surface is greater than its motion);
- Independently moving objects will either not be detected, or will be detected inaccurately.

We are currently investigating the following areas:

- Extending our analysis of connectivity between adjacent EPIs
- Identifying and interpreting spatial and temporal phenomena such as occlusions, shadows, mirrors, and highlights.
- Characterizing the appearance of curved surfaces in EPIs.
- Implementing the analysis of EPIs derived from forward motions.

We plan to write an expanded version of this paper in which we will present our results in these areas.

Appendix A: Lateral-Motion Trajectories

In this appendix we first derive an equation for the trajectory of a point in an EPI constructed from a lateral motion, and then show how to compute the (x,y,z) location of such a point. Figure 24 is a diagram of a trajectory in an EPI derived from the right-to-left motion illustrated in Figure 25. The scanline at t_1 in Figure 24 corresponds to the epipolar line l_1 in Figure 25. Similarly, the scanline at t_2 corresponds to the epipolar line l_2. (Recall that the EPI is constructed by extracting one line from each image taken by the camera as it moves along the line joining c_1 and c_2. Since the images are taken very close together in time, there would be several images taken between c_1 and c_2. However, to simplify the diagram none of these is shown.) The point (u_1, t_1) in the EPI corresponds to the point (u_1, v_1) in the image taken by the camera at time t_1 and position c_1. Thus, as the camera moves from c_1 to c_2 in the time interval t_1 to t_2, the scene point *moves* in the EPI from (u_1, t_1) to (u_2, t_2). The intent of this section is to characterize the shape of this trajectory and then compute the three-dimensional position of the corresponding scene point, given the focal length of the camera, the camera speed, and the coordinates of points along the trajectory.

For our analysis we define a left-handed coordinate system that is centered on the initial position of the camera (i.e., c_1 in Figure 25). The shape of the trajectory can be derived by analyzing the geometric relationships in the epipolar plane that passes through P. Figure 26 is a diagram of that plane.

Given the speed of the camera, s, which is assumed to be constant, the distance from c_1 to c_2, Δx, can be computed as follows:

$$\Delta x \;=\; s\,\Delta t \tag{1}$$

where Δt is $(t_2 - t_1)$. By similar triangles

$$\frac{u_1}{h} = \frac{x}{D} \tag{2}$$

$$\frac{u_2}{h} = \frac{\Delta x + x}{D} \tag{3}$$

where u_1 and u_2 have been converted from pixel values into distances on the image plane, h is the distance from the lens center to the epipolar line in the image plane, x is the x-coordinate of P in the scene coordinate system, and D is the distance from P to the line joining the lens centers. Since h is the hypotenuse of a right triangle, it can be computed as follows:

$$h = \sqrt{f^2 + v_1^2}, \tag{4}$$

where f is the focal length of the camera. From 2 and 3 we get

$$\Delta u = (u_2 - u_1) = \frac{h(\Delta x + x)}{D} - \frac{h\,x}{D} = \frac{h}{D}\Delta x \tag{5}$$

Thus, Δu is a linear function of Δx. Since Δt is also a linear function of Δx, Δt is linearly related to Δu, which means that trajectories in an EPI derived from a lateral motion are straight lines.

The (x, y, z) position of P can be computed by scaling u_1, v_1, and f appropriately. From 5 we define

$$m = \frac{D}{h} = \frac{\Delta x}{\Delta u} \tag{6}$$

which represents the slope of the trajectory computed in terms of the distance traveled by the camera (Δx as opposed to Δt) and the distance the point moved along the epipolar line (i.e., Δu). From similar triangles

$$(x, y, z) = \left(\frac{D}{h}u_1, \frac{D}{h}v_1, \frac{D}{h}f\right) \tag{7}$$

which means that

$$(x, y, z) = (mu_1, mv_1, mf) \tag{8}$$

If the first camera position, c_1, on an observed trajectory is different from the camera position, c_0, that defines a global camera coordinate system, the x coordinate can be adjusted by an amount equal to the distance traveled from c_0 to c_1. Thus,

$$(x, y, z) = ((t_1 - t_0)s + mu_1, mv_1, mf) \tag{9}$$

where t_0 is the time of the first image and s is the speed of the camera. This correction is equivalent to computing the x intercept of the line and using it as the first camera position. Therefore, for a lateral motion, the trajectories are linear and the (x, y, z) coordinates of the points can be easily computed from the slopes and intercepts of the lines.

Appendix B: Forward-Motion Trajectories

The derivation of the form of a trajectory produced by a forward motion is similar to the one used for lateral motion. Figure 27 is a diagram of a trajectory in an EPI derived from a sequence of images taken by a camera moving in a straight line at a fixed orientation relative to the principal axis of the camera (see Figure 28). Without loss of generality we have rotated the image plane coordinate systems in a uniform way so that the epipoles are on the u axes. The EPI in Figure 27 was constructed by extracting pixel intensities along epipolar lines in the images shown in Figure 28 and inserting them as scanlines in Figure 27. For example, epipolar line l_1 was placed at t_1, l_2 was placed at t_2, and so on. The point (w_1, t_1) in the EPI corresponds to the point (u_1, v_1) in the image taken at time t_1 and position c_1. Thus, as the camera moves from c_1 to c_2 over the time interval t_1 to t_2, the scene point *moves* in the EPI from (w_1, t_1) to (w_2, t_2). Our goal is to characterize the shape of this trajectory, and then compute the three-dimensional position of the corresponding scene point, given the focal length of the camera, the camera speed, the angle between the camera's axis and the direction of motion (θ), and the coordinates of points along the trajectory.

As before, we define a left-handed coordinate system that is centered on the initial position of the camera (i.e., c_1 in Figure 28). The shape of the trajectory can be derived by examining the geometric relationships in the epipolar plane that passes through P. Figure 29 is a diagram of that plane.

Given the speed of the camera, s, which is assumed to be constant, the distance from c_1 to c_2, Δe, can be computed as follows:

$$\Delta e = s\,\Delta t \tag{10}$$

where Δt is $(t_2 - t_1)$. By similar triangles

$$\frac{w_1}{h} = \frac{C}{e} \tag{11}$$

and

$$\frac{w_2}{h} = \frac{C}{(e - \Delta e)} \tag{12}$$

where w_1 and w_2 are distances on the image plane, h is the distance from the lens center to the epipole, C is the distance from P to the line joining the lens centers measured in a plane parallel to the image planes, and e is the distance along the line joining the lens centers from c_1 to the plane passing through P and parallel to the image planes. Since h is the hypotenuse of a right triangle (see Figure 28), it can be computed as follows:

$$h = \frac{f}{cos\theta} \tag{13}$$

where f is the focal length of the camera. From 11 and 12 we get

$$\Delta w = (w_2 - w_1) = \frac{hC}{(e - \Delta e)} - \frac{hC}{e} = \frac{hC\Delta e}{e(e - \Delta e)} \tag{14}$$

which can be rewritten as

$$e\,\Delta w\,\Delta e \;-\; e^2\Delta w \;+\; hC\Delta e \;=\; 0. \tag{15}$$

Using 10 to express Δe in terms of Δt, this becomes

$$se\Delta w\Delta t \;-\; e^2\Delta w \;+\; shC\Delta t \;=\; 0. \tag{16}$$

which defines a hyperbola whose asymptotes are the lines $w = 0$ and $t = e/s$ (see Figure 30). Thus, the trajectory is a hyperbola in which the point P appears arbitrarily close to the epipole when the camera is far away from it (as one would expect), and the projection of P moves away from the epipole at an increasing rate as the camera gets closer to it. This relationship agrees intuitively with the fact that a projective transformation involves a $1/z$ factor, which makes u a hyperbolic function of z.

Equation 14 can be used to compute z. First, rewrite it as follows:

$$\Delta w = \frac{hC}{(e - \Delta e)}\frac{1}{e}\Delta e \tag{17}$$

Then using Equation 12 and

$$e = \frac{z}{cos\theta} \tag{18}$$

we get

$$\Delta w = \frac{w_2\, cos\theta\, \Delta e}{z} \tag{19}$$

or

$$z = \frac{w_2\, cos\theta\, s\Delta t}{\Delta w} \tag{20}$$

Notice that it is NOT necessary to determine the coefficients of the hyperbola in order to compute z. Two points on the trajectqry are sufficient to compute Δt and Δw, which in turn, are sufficient to compute z. Also notice, however, that it is easy to fit an hyperbola of this type because it is in the simple form

$$\Delta w\Delta t \;+\; a\Delta w \;+\; b\Delta t \;=\; 0, \tag{21}$$

which is linear with respect to the coefficients a and b. This type of fitting provides a way to increase the precision with which the scene points are located.

The expression for z in Equation 20 does not apply when $\theta = 90°$, but that is the lateral motion case covered earlier. Thus, the trajectories are always hyperbolas; they just happen to degenerate into straight lines when $\theta = 90°$, which corresponds to the case in which the epipoles are not in the image plane, but rather lie at infinity.

The x and y coordinates for P can be computed by scaling z appropriately:

$$(x, y) = (\frac{u_1}{f}z, \frac{v_1}{f}z) \tag{22}$$

Recall that u_1 and v_1 are measured in a rotated-image-plane coordinate system that was set up to place the epipole on the u axis. Therefore, in addition to converting pixel values to a standard metric, such as meters, the image coordinates of a point must be rotated about the principal axis before they can be inserted into Equation 22. To compute a world-centered position for P, the (x, y, z) position computed by Equations 20 and 22 has to be transformed for the initial position of the camera along the path.

References

[1] "Disparity Analysis of Images," S. T. Barnard and W. B. Thompson, *IEEE Trans., PAMI,* **Vol 2, No 4,** 1980.

[2] "A Discrete Spatial Representation for Lateral Motion Stereo," N. J. Bridwell and T. S. Huang, *Computer Vision, Graphics, and Image Processing,* Vol **21,** 1983.

[3] "Monocular Depth Perception from Optical Flow by Space Time Signal Processing," B. F. and Hilary Buxton, *Proceedings of the Royal Society of London, B.,* Vol **218,** 1983.

[4] "Computation of optic flow from the motion of edge features in image sequences," B. F. and H. Buxton, *Image and Vision Computing,* **Vol 2, No 2,** May 1985.

[5] "Detection of Moving Edges,"S. M. Haynes and R. Jain, *Computer Vision,Graphics, and Image Processing,* **Vol 21, No 3,** 1983.

[6] "Computations Underlying the Measurement of Visual Motion," E. C. Hildreth, *Artificial Intelligence,* Vol **23,** 1984.

[7] "Theory of Edge Detection," D. C. Marr and E. Hildreth, *Proceedings of the Royal Society of London,* B **207,** 1980.

[8] "Depth Measurement from Motion Stereo," Ramakant Nevatia, *Computer Graphics and Image Processing,* **5,** 1976.

[9] "An Iterative Procedure for the Polygonal Approximation of Plane Curves," U. Ramer, *Computer Graphics and Image Processing* Vol **1,** 1972.

[10] *The Interpretation of Visual Motion,* S. Ullman, MIT Press, Cambridge, Mass., 1979.

[11] "Determining 3-D Motion and Structure of a Rigid Body Using the Spherical Projection," B. L. Yen and T. S. Huang, *Computer Graphics and Image Processing,* Vol **21,** 1983.

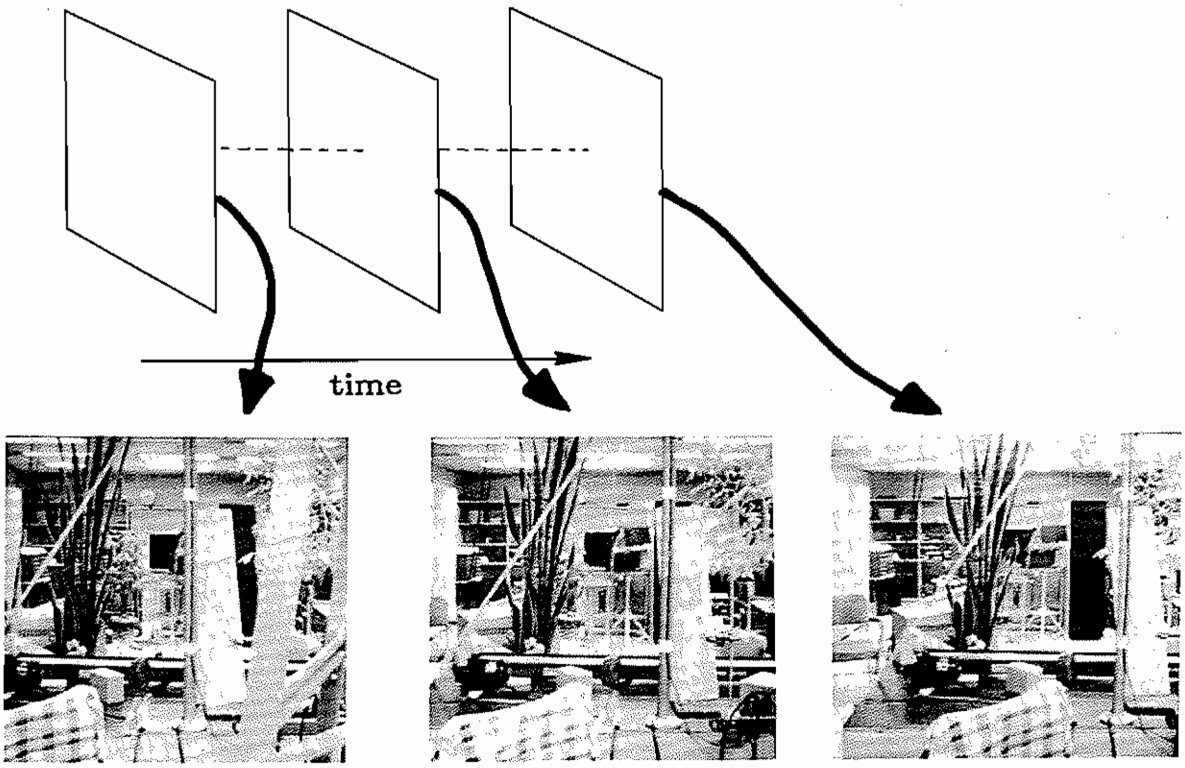

Fig. 1. Typical image separation

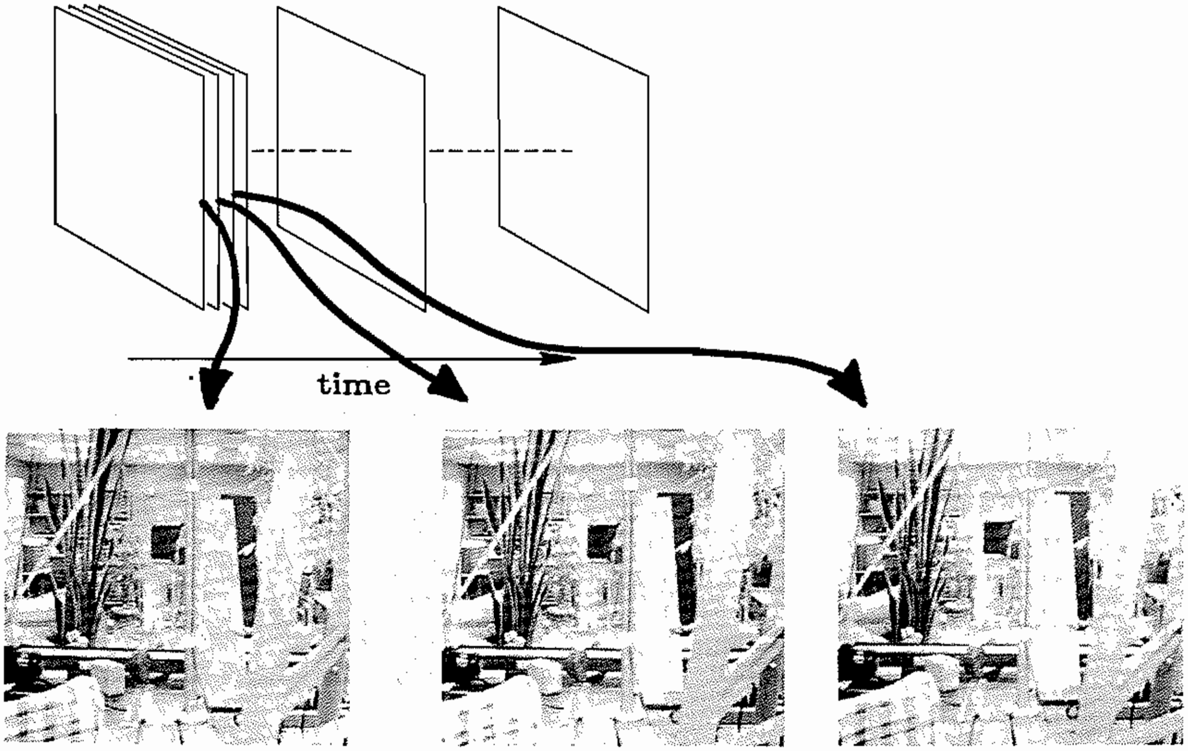

Fig. 2. Close sampling image separation

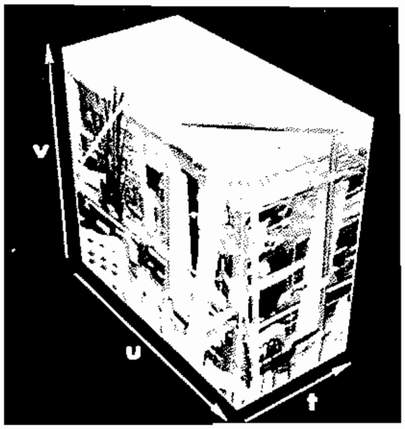

Fig. 3. Spatio-temporal solid of data

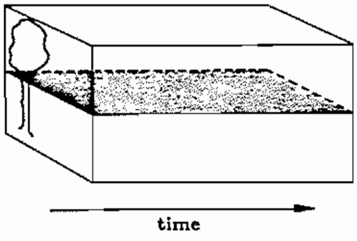

Fig. 4. Slice of the solid of data

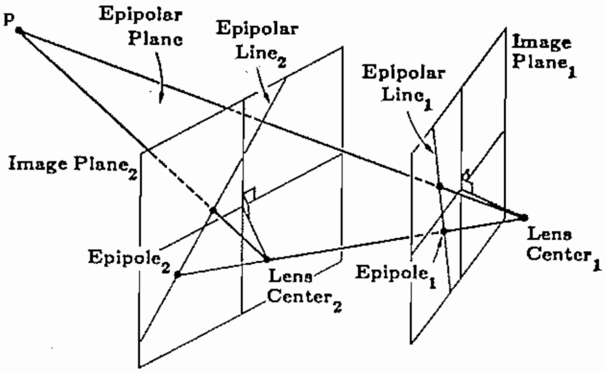

Fig. 5. General stereo configuration

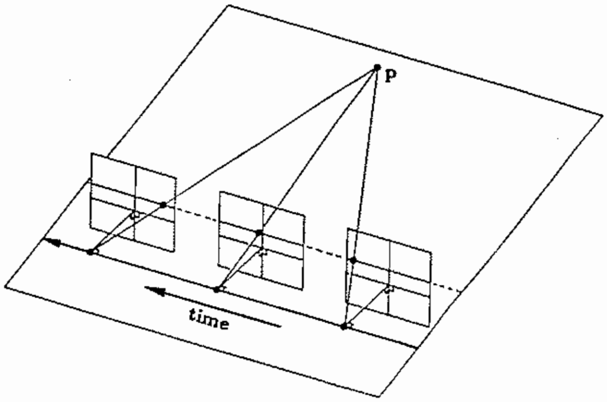

Fig. 6. Right-to-left motion

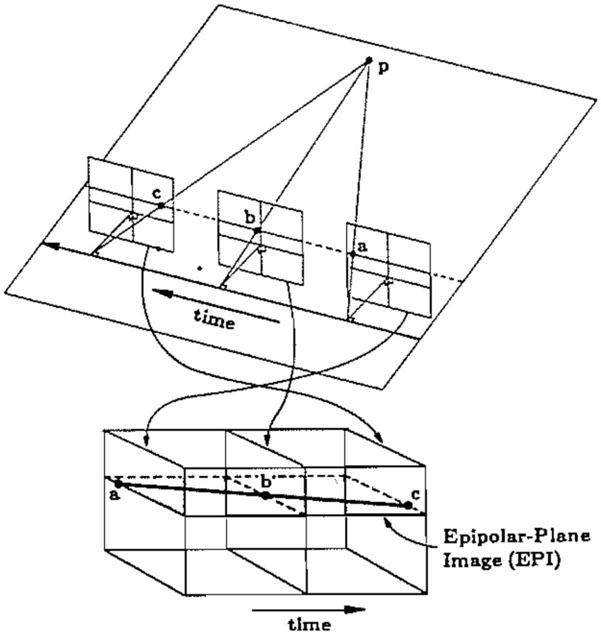

Fig. 7. Right-to-left motion with solid

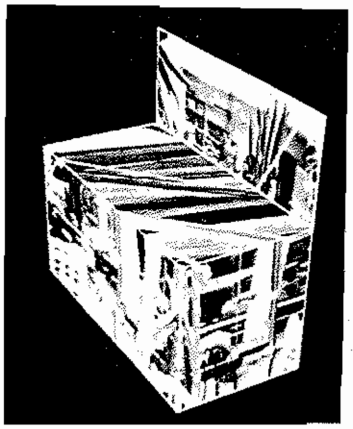

Fig. 8. Sliced solid of data

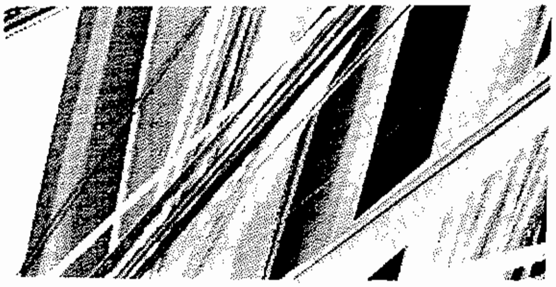

Fig. 9. Frontal view of the EPI

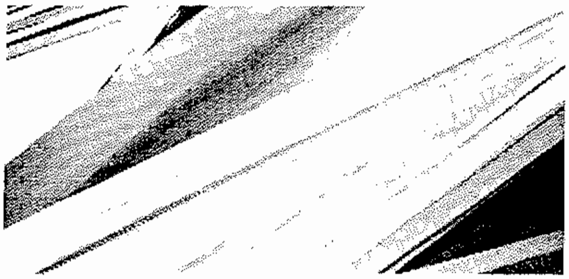

Fig. 10. A second EPI

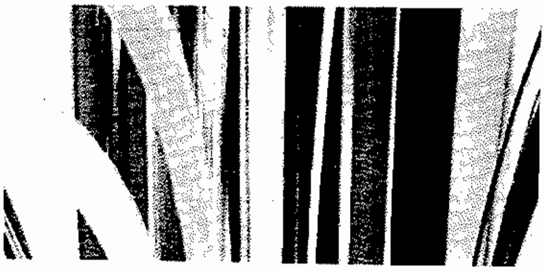

Fig. 11. EPI from forward motion

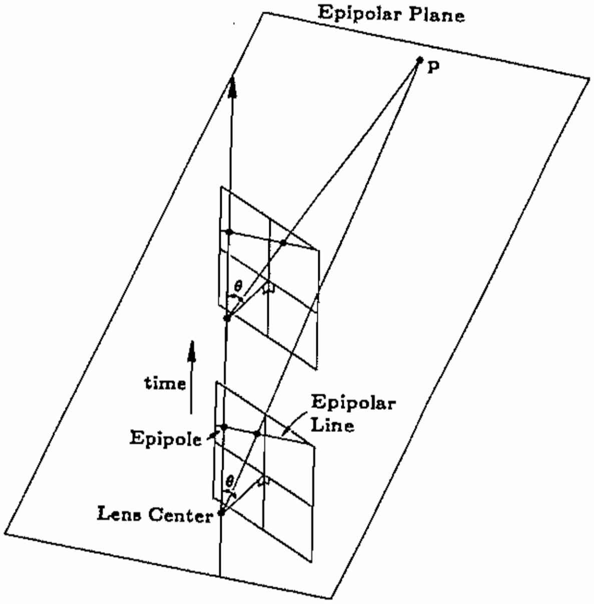

Fig. 12. Forward motion

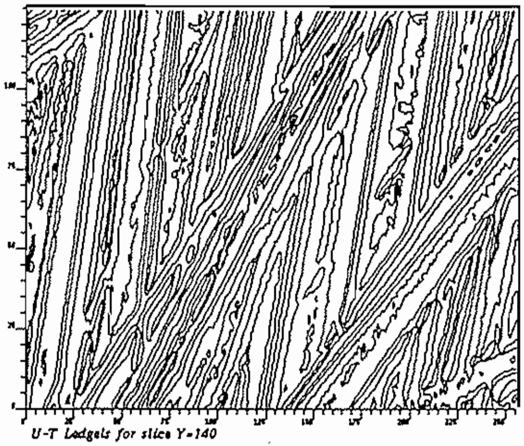

Fig. 13. Edge features in EPI

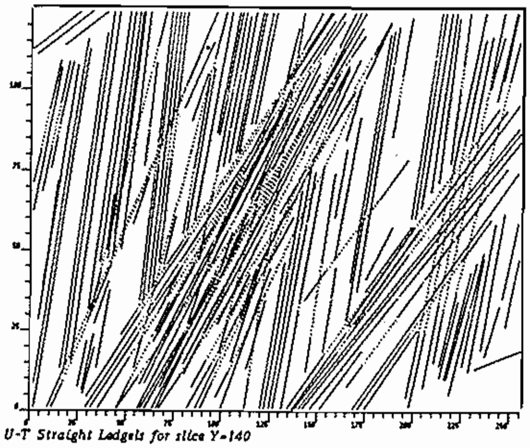

Fig. 14. Straight lines

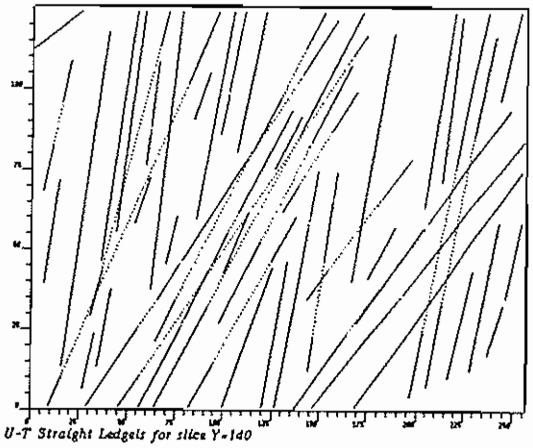

Fig. 15. Linked peak lines

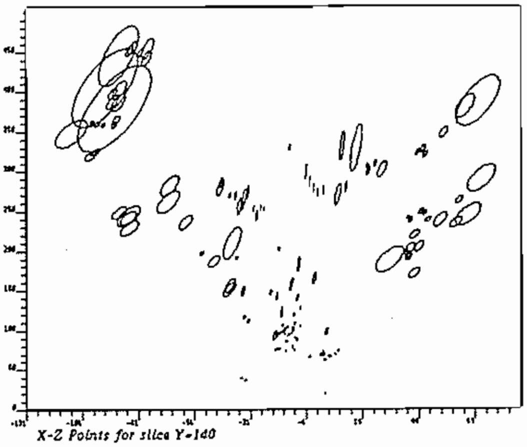

Fig. 16. xz locations

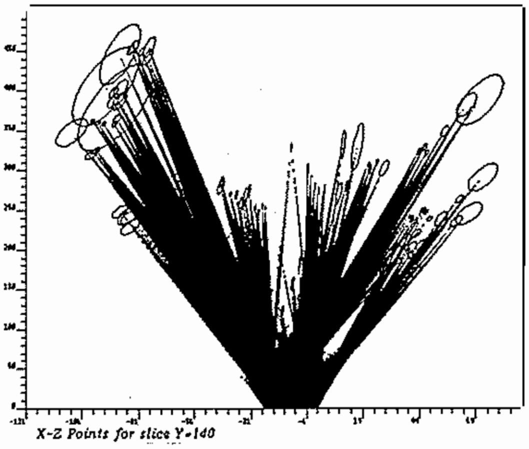

Fig. 17. Free space

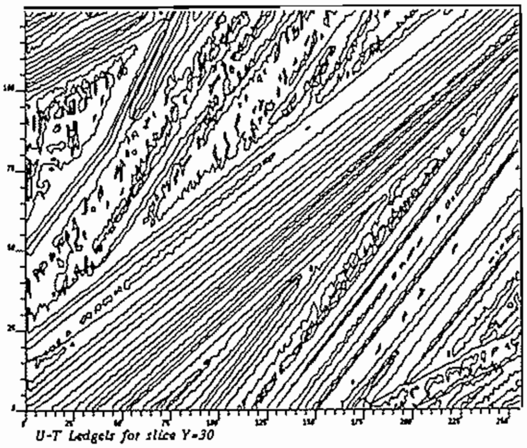

Fig. 18. Edge features in EPI

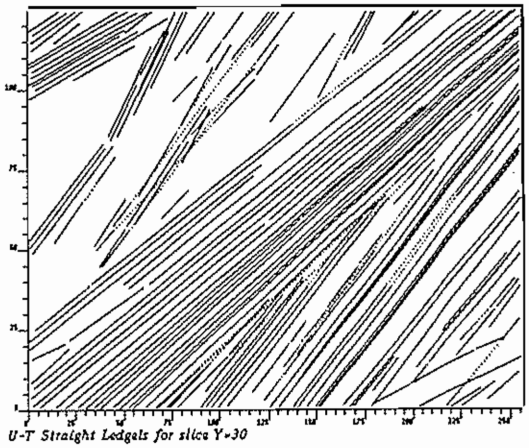

Fig. 19. Straight lines

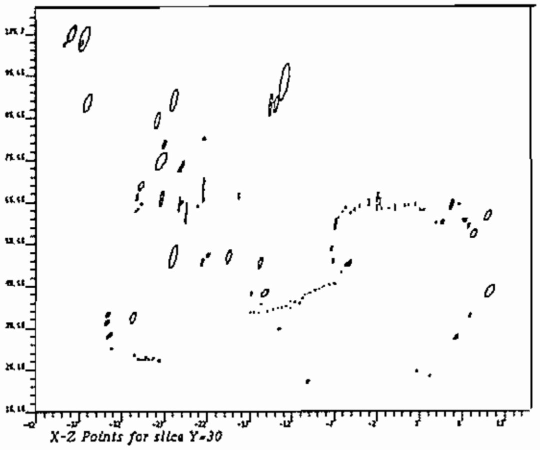

Fig. 20. xz locations

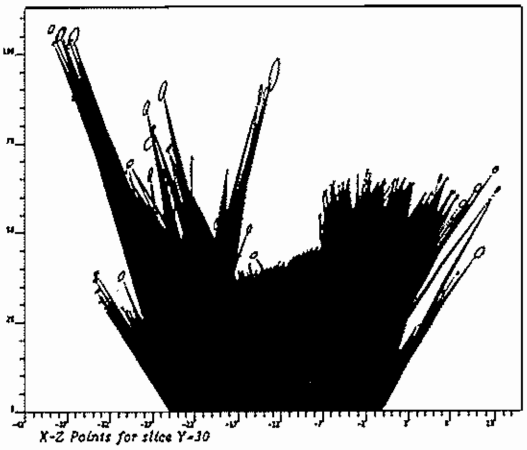

Fig. 21. Free space

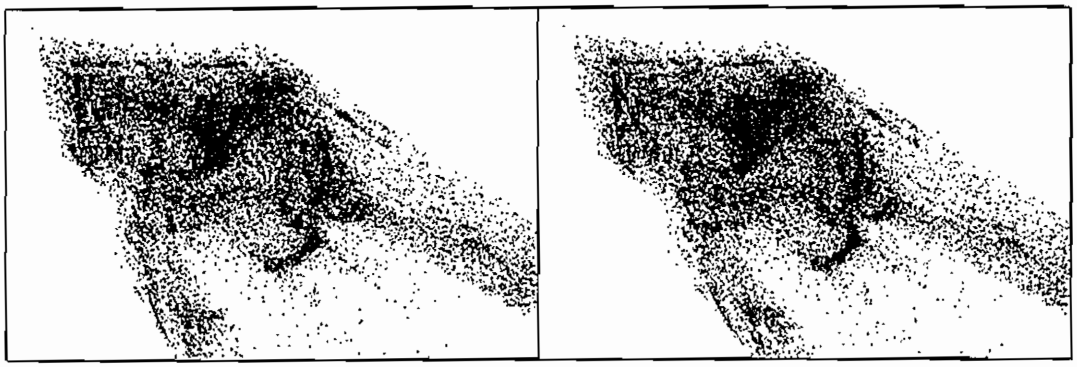

Fig. 22. Stereo display of all x-y-z points

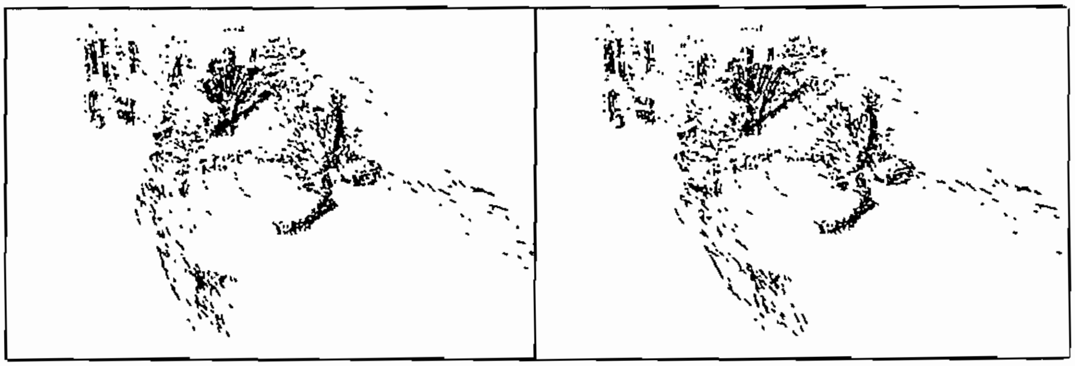

Fig. 23. Display of linked x-y-z points

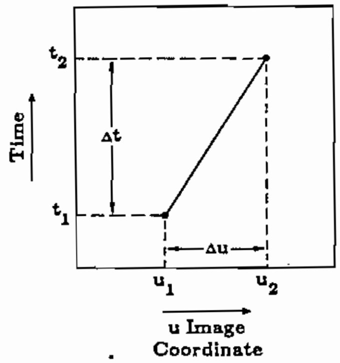

Fig. 24. Lateral motion EPI

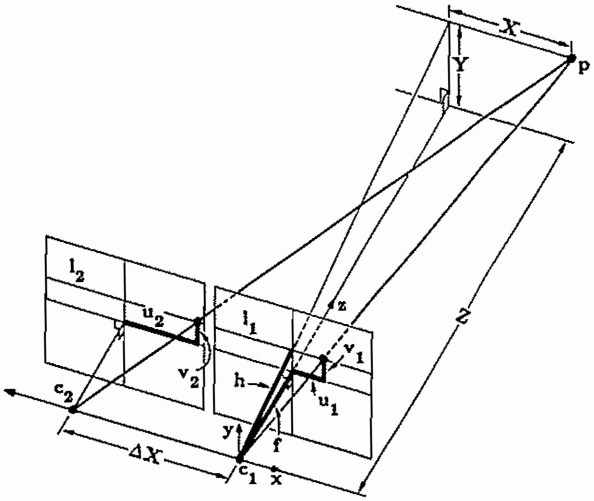

Fig. 25. Lateral motion geometry

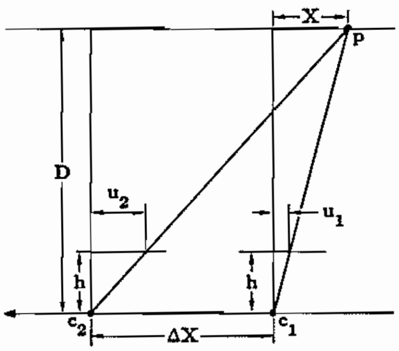

Fig. 26. Lateral motion epipolar geometry

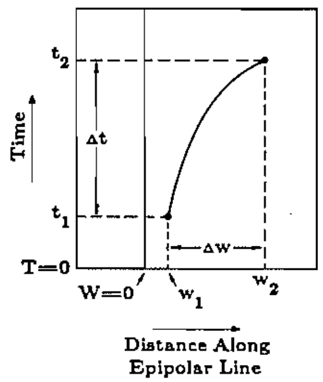

Fig. 27. Forward motion EPI

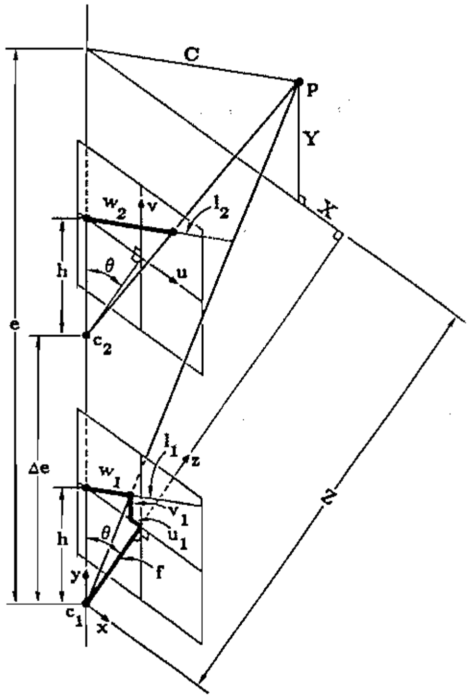

Fig. 28. Forward motion geometry

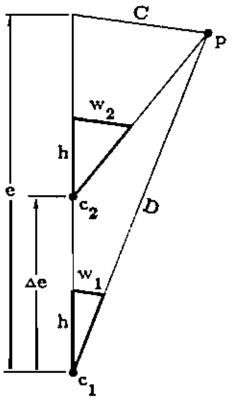

Fig. 29. Forward motion epipolar plane

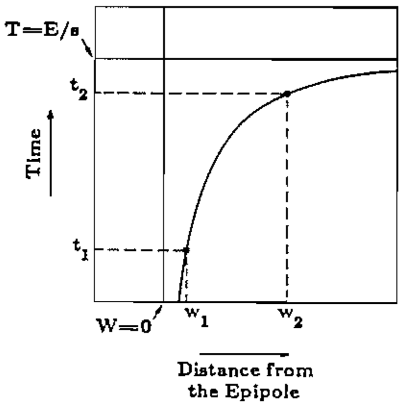

Fig. 30. Asymptotes for the hyperbola